NeuroImage: Clinical 14 (2017) 269–276

Contents lists available at ScienceDirect

NeuroImage: Clinical

journal homepage: www.elsevier.com/locate/ynicl

Longitudinal evaluation of cerebral and spinal cord damage in Amyotrophic Lateral Sclerosis

Milena de Albuquerque[1], Lucas Melo T Branco[1], Thiago Junqueira R. Rezende, Helen Maia Tavares de Andrade, Anamarli Nucci, Marcondes Cavalcante França Jr*

Department of Neurology and Neuroimaging Laboratory, School of Medical Sciences, University of Campinas – UNICAMP Rua Tessália Vieira de Camargo, 126, Cidade Universitaria "Zeferino Vaz" Campinas, SP 13083-887, Brazil

ARTICLE INFO

Article history:
Received 20 November 2016
Received in revised form 19 January 2017
Accepted 23 January 2017
Available online 24 January 2017

Keywords:
MRI
Amyotrophic Lateral Sclerosis
Cortical thickness
TBSS
Spinal cord

ABSTRACT

Objective: To evaluate MRI-based parameters as biomarkers of Amyotrophic Lateral Sclerosis (ALS) progression.
Methods: Twenty-seven patients and 27 controls performed two clinical and MRI acquisitions 8 months apart. ALSFRS-R scale was used to quantify disease severity at both time points. Multimodal analyses of MRI included cortical thickness measurements (FreeSurfer software), analysis of white matter integrity using diffusion-tensor imaging (tract-based spatial statistics-TBSS) and measurement of cervical spinal cord cross-sectional area (SpineSeg software). All analyses were corrected for multiple comparisons. The standardized response mean (SRM = mean score change / standard deviation of score change) was calculated for all methods herein employed and used for comparison purposes.
Results: There were 18 men and mean age at first examination was 51.9 years. Mean ALSFRS-R scores at baseline and follow-up were 34.0 and 29.0, respectively. There was no region with progressive cortical thinning, but there was significant brainstem volumetric reduction ($p = 0.001$). TBSS analyses revealed progressive increase of AD (axial diffusivity) and MD (mean diffusivity) at the corpus callosum ($p < 0.05$), whereas SpineSeg showed progressive cord area reduction ($p = 0.002$). Cervical spinal cord cross-sectional area reduction was the only MRI parameter that correlated with ALSFRS-R change ($r = 0.309$, $p = 0.038$). SRM for ALSFRS-R was 0.95, for cord area 0.95, for corpus callosum AD 0.62 and MD 0.65, and for brainstem volume 0.002.
Conclusions: Structural MRI is able to detect short term longitudinal changes in ALS. Cervical spinal cord morphometry is a promising neuroimaging marker to assess ALS course.

1. Introduction

Biomarkers are needed to assess prognosis and to improve the design of clinical trials for patients with Amyotrophic Lateral Sclerosis (ALS) (Kiernan et al., 2011; Turner et al., 2009; Turner et al., 2013). Magnetic Resonance Imaging (MRI) has emerged as a promising candidate (Foerster et al., 2013; Holtbernd and Eidelberg, 2014; da Rocha and Maia Júnior, 2012, Salvatore et al., 2015; Turner et al., 2012) and it enabled so far the assessment of white matter (WM) and grey matter (GM) impairment in ALS, showing damage to corticospinal tracts (CST) (Roccatagliata et al., 2009; Walhout et al., 2014), non-motor areas (Agosta et al., 2012; Bede et al., 2013; De Albuquerque et al., 2016, Westeneng et al., 2015) and Spinal Cord (SC) (Branco et al., 2014). However, most published studies are cross sectional and the longitudinal studies available are mostly unimodal (Verstraete et al., 2012, Zhang et al., 2011). Some researchers performed multimodal and longitudinal MRI evaluation, but simultaneous brain and SC evaluation are rare. On a recent review (Schuster et al., 2015), about 85% of the longitudinal studies based their conclusions on a single brain imaging measure. Agosta et al. (2009) performed a follow-up study using DTI of brain and cervical cord MRI of 17 patients. They found decreased cord area and mean FA, but brain CST diffusivity measurements remained stable over time in ALS patients and did not correlate with cord damage. Menke et al. (2014) studied prospectively 27 patients and found progression more evident at the GM (including frontotemporal and basal ganglia) rather than the WM (corpus callosum and left CST). Another longitudinal study with 17 patients found widespread volumetric reduction in GM, but DTI abnormalities localized mainly into the bilateral frontal lobes after 6 months (Senda et al., 2011). The results are

* Corresponding author at: Department of Neurology, University of Campinas – UNICAMP, Rua Tessália Vieira de Camargo, 126, Cidade Universitaria "Zeferino Vaz" Campinas, SP 13083-887, Brazil. Tel.: +55 19 3521 9217.
E-mail addresses: mcfrancajr@uol.com.br, mcfrancajr@gmail.com (M.C. França Jr).
[1] Both authors contributed equally to this work.

http://dx.doi.org/10.1016/j.nicl.2017.01.024

conflicting, especially regarding whether there is progression amenable to detection within short follow up times. Thus, reliability of MRI parameters as prognostic markers still needs to be elucidated.

Recently, a new longitudinal study (Cardenas-Blanco et al., 2016) evaluated 34 patients with multimodal brain MRI parameters and clinical scores, finding DTI to be a superior imaging marker, but less sensitive than clinical score for monitoring decline over time. In this scenario, we designed this study to evaluate how different MRI-based parameters change over time, to compare them and to assess whether they correlate with clinical deterioration. We were primarily interested in investigating whether SC morphometry is more sensitive to detect longitudinal changes than cranial measurements, such as volumetry, cortical thickness and DTI-based parameters.

2. Materials and methods

2.1. Subjects selection and clinical evaluation

Sixty-three non-demented sporadic patients with ALS diagnosed according to the El Escorial criteria (Brooks et al., 2000) regularly followed at UNICAMP hospital were enrolled. Imaging findings at baseline were compared with a group of 64 healthy controls without personal or family history of neurological disorders. None of the individuals was younger than 18 years or had other concomitant neurological disorders. All patients were genotyped for C9orf72 status and tested negative for GGGGCC expansions. Specifically for DTI analyses, we had to exclude 10 patients and 7 healthy controls due to severe motion artifacts on DTI images (clinical and demographic of these patients were similar to the whole ALS cohort – n = 63). Twenty-seven patients performed a second evaluation after 8 months. Twenty-seven healthy controls also had a follow-up MRI, which we used for comparison with the ALS follow-up group. All patients underwent detailed clinical examination with Amyotrophic Lateral Sclerosis Functional Rating Score-Revised (ALSFRS-R) (Cedarbaum et al., 1999) assessment at both time points by two examiners (MdeA, HMTdeA).

2.2. Standard protocol approvals, registrations, and patient consents

This study was approved by UNICAMP research ethics committee (#270/2011) and written informed consent was obtained from all participants.

2.3. MRI acquisition

All participants underwent MRI on a 3T scanner. Routine T1 and T2 weighted sequences were performed to exclude unrelated abnormalities. Volumetric T1 images of the brain and spinal cord were acquired for FreeSurfer and SpineSeg analyses using a standard 8-channel head coil: sagittal orientation, voxel matrix 240 × 240 × 180, voxel size 1 × 1 × 1 mm^3·TR/TE 7/3.201 ms, flip angle 8°. For DTI analyses, we used a spin echo DTI sequence: 2 × 2 × 2 mm^3 acquiring voxel size, interpolated to 1 × 1 × 2 mm^3; reconstructed matrix 256 × 256; 70 slices; TE/TR 61/8500 ms; flip angle 90°; 32 gradient directions; no averages; max b-factor = 1000s/mm^2.

2.4. MRI analyses

The design of the study is shown in Fig. 1.

2.4.1. Cerebral GM analyses

2.4.1.1. Cross sectional

2.4.1.1.1. FreeSurfer. FreeSurfer software v.5.3 was employed to assess GM volume and thickness. Processing steps (Fischl and Dale, 2000; Fischl et al., 2002) included correction for magnetic field inhomogeneity, alignment to a specific atlas (Talairach and Tournoux, 1988), skull removal and segmentation of voxels into GM, WM and CSF. Cortical thickness (CT) was then calculated based in the shortest distance of two surfaces: the interface between GM and WM and the pial one. A Gaussian filter of 10 mm FWHM was used for smoothing in all analyses. Estimated Intracranial Volume (eTIV) and the volume of subcortical structures were also determined (Buckner et al., 2004). We employed

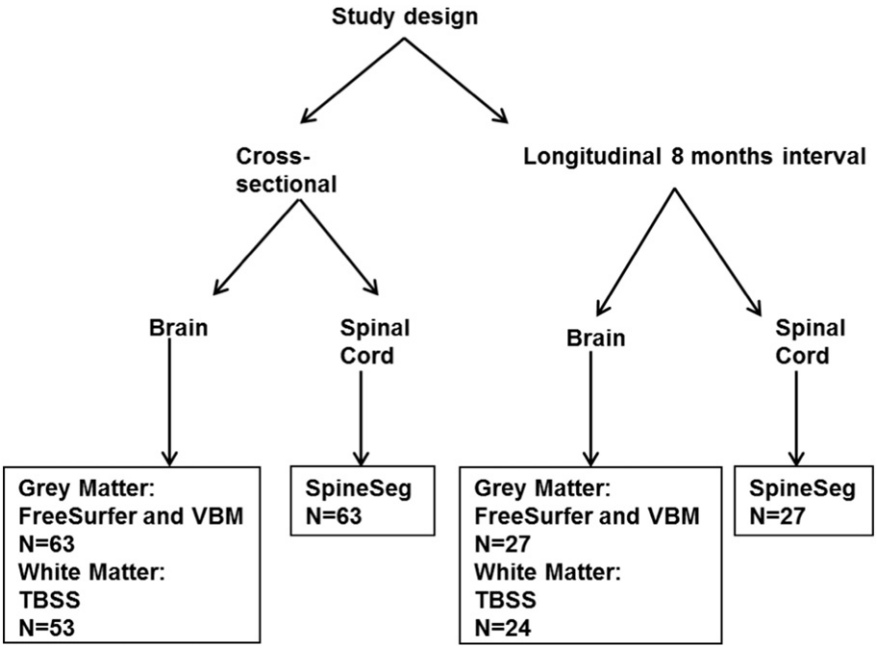

Fig. 1. Design of the study.

a General Linear Model (GLM) using age and gender as covariates to assess between-groups CT differences in brain regions according to the Desikan and Detrieux Atlas (Desikan et al., 2006). Regarding subcortical volumes, we also compared groups using a GLM, but taking age, gender and also eTIV as covariates. In order to correct the results for multiple comparisons, we used FDR-corrected p-values of 0.05 for all CT and volume analyses. This analysis was performed on SYSTAT software v13.0 (San José, CA).

2.4.1.1.2. Voxel-based morphometry (VBM). We used the SPM 8 software (Wellcome Department of Imaging Neuroscience, London, England, www.fil.ion.ucl.ac.uk) and VBM 8 (http://dbm.neuro.uni-jena.de/vbm8/) running on MATLAB 8.0 to perform automated pre-processing spatial normalization, segmentation, modulation and smoothing. Spatial normalization was accomplished with the DARTEL algorithm (Ashburner, 2007) and processed images were compared using a voxel-wise statistical analysis (Ashburner and Friston, 2000). In order to display the results and precise their anatomical location we used an SPM extension, XJVIEW (http://www.alivelearn.net/xjview/). Groups were compared using a *t*-test and results were corrected for multiple comparisons using false discovery rate (FDR) ($p = 0.05$) and cluster size >30 voxels.

2.4.1.2. Longitudinal

2.4.1.2.1. FreeSurfer. We employed the longitudinal FreeSurfer pipeline to evaluate longitudinal CT change. To accomplish that, it co-registers all time-point scans for each subject using a robust and inverse consistent registration algorithm (Reuter et al., 2010) in order to create an unbiased subject-specific template (Reuter and Fischl, 2011) keeping saved common information from all time-points (e.g. skull-stripping, Talairach transformation and parcellation). Then, several steps in the longitudinal processing stream are initialized from subject-specific template. This approach has been shown to increase reliability and statistical power (Reuter et al., 2012). The statistical analysis was performed using a linear mixed effect model (LME) (Bernal-Rusiel et al., 2013) and taking age at baseline and gender as covariates. p values <0.05 (FDR corrected) were considered significant.

In order to investigate possible correlations between CT change and clinical data variation, we used Pearson coefficients with Dunn-Sidak correction for multiple comparisons.

2.4.1.2.2. VBM. Voxel-wise grey matter differences were examined using a flexible factorial design assessing time (baseline and follow-up) versus groups differences. We considered significant results at $p < 0.05$ (FDR-corrected) and cluster sizes >30 voxels (Gläscher, 2008).

2.4.2. WM analyses

2.4.2.1. Cross sectional. FMRIB toolbox on FSL v.4.1.4 was used to create maps of fractional anisotropy (FA), mean diffusivity (MD), radial diffusivity (RD) and axial diffusivity (AD). Then, it was used in the comparison between patients and controls, performed with the tract based spatial statistics (TBSS) algorithm as described elsewhere (Smith et al., 2006). A two-sample *t*-test was employed to compare patients and controls regarding FA, MD, AD and RD parameters, with cluster-based correction for multiple comparisons (p-value < 0.05). We employed a GLM to investigate possible correlations with clinical data using Threshold Free Cluster-Enhancement (TFCE) correction (Smith and Nichols, 2009). Johns Hopkins white matter DTI-based atlas (available in the FSL software) was employed to identify WM tracts with abnormal findings.

2.4.2.2. Longitudinal. Our longitudinal TBSS pipeline follows the steps proposed by Menke et al. (2014). FA maps of each patient in native space were linearly registered into halfway space and averaged. To accomplish that, both images were linearly registered to each other, and then the transformation matrix into halfway space was calculated. This transformation was applied in both images, thus resulting in an average image. This method was also applied to MD, AD and RD maps in native space for both times points. Afterwards, we ran the standard TBSS protocol, and statistical analysis was performed using a paired two-sample *t*-test, with TFCE (Smith and Nichols, 2009) correction (alpha = 0.05). The same procedure was performed with control images. We assessed possible correlations with clinical deterioration using a GLM with TFCE correction.

We then applied a mask on the results of the TBSS on the regions with abnormal DTI results to extract AD and MD quantitative data for each patient. This was later employed to calculate the mean score change of these parameters.

2.4.3. SC morphometry

2.4.3.1. Cross sectional. SpineSeg software was used to estimate cervical SC area and eccentricity (Bergo et al., 2012). This tool resamples the MR images correcting for variations in imaging angle and neck position. Cross-sections of the spinal cord are segmented based on a semi-automatic protocol, and the best ellipse corresponding to SC on the selected level is fitted (Fig. 2). Then, SpineSeg provides measurements of spinal cord area (CA) and spinal cord eccentricity (CE) based on the fitted ellipse for chosen level. These measures were performed at the higher section of the intervertebral disc between C2 and C3 using standard structural brain MRI acquisition (Branco et al., 2014). CE was taken as an estimate of the antero-posterior flattening of the cord. All measurements were performed by a single investigator who was blind to the clinical status of subjects (LMTB). We used the mean values obtained from three consecutive levels measurements at the mid-section of the intervertebral disc between C2 and C3 in each subject (Branco et al., 2014). This level was chosen because it includes the cervical intumescence thus making the cord larger and enabling easier detection of atrophy. In addition, it is the region most commonly employed for MRI based CA measurements, which permits comparison of our own data with previous reports (Chevis et al., 2013). Group comparison of CA and CE parameters was done using an ANCOVA with age at baseline and gender as covariates. Correlation of ALSFRS-R score and CA was assessed using Pearson correlation, since our data had normal distribution (Shapiro-Wilk test $p = 0.116$).

2.4.3.2. Longitudinal. We evaluated longitudinal CA change in control and ALS groups using a linear mixed model taking into account the group vs time interaction. Age at baseline, gender and inter-scan interval were used as covariates in this model. Longitudinal CA change in the ALS group was correlated to ALSFRS-R, motor subscore and upper motor neuron scale changes using Spearman coefficient. All statistical analyses were performed in SPSS v.20 software.

2.4.4. Change rate among different methods

The standardized response mean (SRM), expressed as mean score change/standard deviation (SD) of score change is reported as effect size index to enable a comparison between scales/markers. Values of 0.20, 0.50, and 0.80 are considered to represent small, moderate, and large changes (Kazis et al., 1989). This was calculated for all methods herein employed, seeking for the most sensitive to describe disease progression.

3. Results

3.1. Clinical and demographic data

Clinical and demographic data of enrolled individuals are shown in Table 1. None of the patients had frontotemporal dementia or major behavioural impairment on routine evaluation. Detailed neuropsychological evaluation was available for 14/63 patients, 4 of which had mild behavioural impairment (abnormal scores on at least 2 domains of the neuropsychiatric inventory). None of these 4 patients underwent a

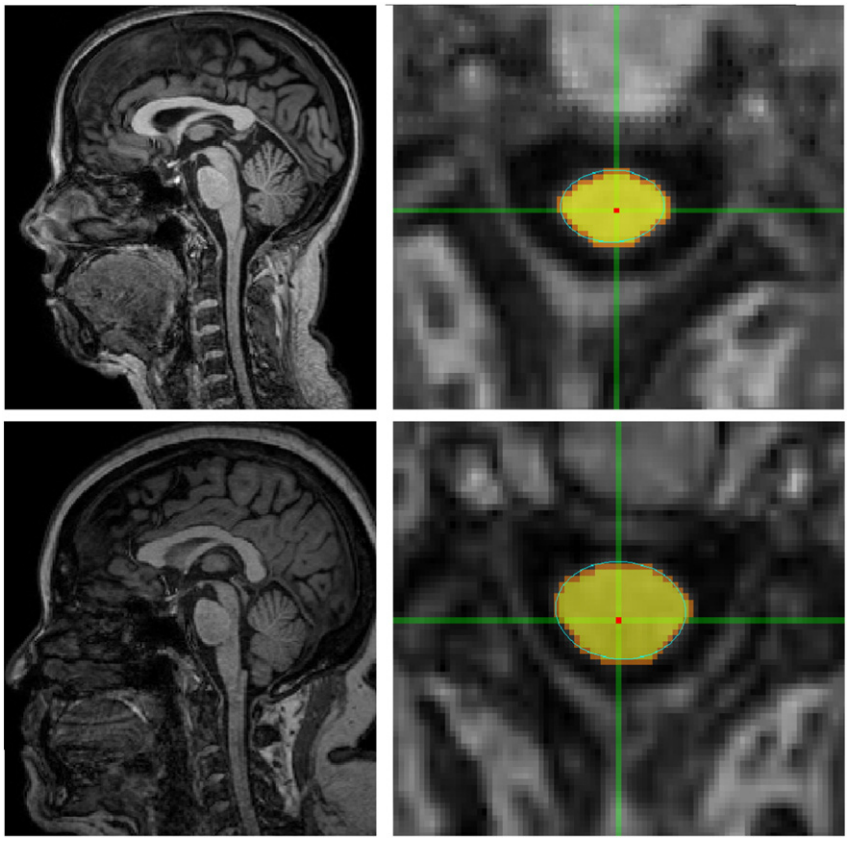

Fig. 2. Layout of the SpineSeg software showing the segmentation of the cervical spinal cord in a patient with ALS (upper lanes) and a healthy control (lower lanes).

second MRI scan. In the follow-up, 16 patients had severe clinical worsening, and were unable to repeat MRI scans, due to respiratory failure ($n = 8$) and death ($n = 8$). Ten patients were lost to follow-up before the second evaluation. Fifteen patients were recently assessed, i.e. <-6 months before statistical analyses, and thus have not performed a follow-up evaluation.

Despite that, it is important to highlight that the clinical and demographic profile of patients that underwent one and two clinical/MRI assessments was similar. Both groups were balanced in terms of age ($p = 0.143$), gender distribution ($p = 0.812$), disease duration ($p = 0.163$), ALSFRS-R score ($p = 0.135$) and ALS subtype ($p = 0.758$). So, we believe that the longitudinal results are representative of the whole cohort despite the smaller cohort size. Regarding age, we acknowledge that there was a significant difference between patients and controls that underwent longitudinal scans ($p = 0.0022$). To minimize the effects of such difference, we included age as a covariate in all statistical analyses.

Table 1
Clinical and demographic data of patients and controls.

		Age onset (y) median (min-max)	Gender (M:F)	Disease duration (mo) Median (min-max)	limb/bulbar onset	El Escorial criteria (definite/probable/possible)	ALSFRS-R median (min-max)
Cross-sectional							
GM analyses	Patient (n = 63)	57 (31–77)	39:24	18 (4–144)	52/11	13/42/7	34 (12–45)
	Control (n = 64)	54.5 (24–82)	38:26	–		–	–
WM analyses	Patient (n = 53)	56 (31–77)	34:19	18.5 (4–144)	43/9	12/35/5	34.5 (12–45)
	Control (n = 57)	55 (24–82)	38:19	–		–	–
Longitudinal							
GM analyses (mean interval between scans: patients = 8.4 months, controls = 12.9 months)	Patient (n = 27)	50 (33–70)	18:9	30.5 (16–150)	23/4	5/19/3	32.5 (11–42)
	Control (n = 27)	41.6 (24–64)	11:16	–		–	–
WM analyses (mean interval between scans: patients = 8.0 months, controls = 11.5 months)	Patient (n = 24)	41 (24–64)	15:9	31(16–150)	22/2	5/18/1	31 (11–42)
	Control (n = 20)	40.5 (24–64)	11:9	–		–	–

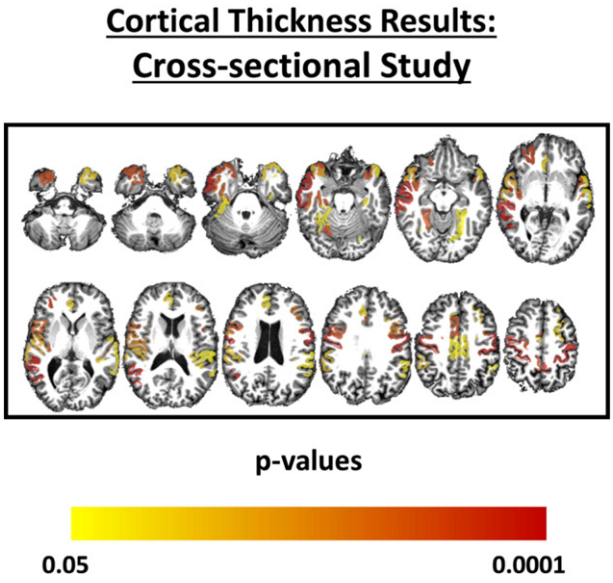

Fig. 3. Areas with reduced cortical thickness in patients with ALS compared to healthy controls. The color coded bar represents the corrected p-values for each cortical region.

3.2. Cerebral GM

3.2.1. Cross-sectional

At baseline, group comparison showed reduced CT in the ALS group, especially at paracentral, precentral and temporal areas (Fig. 3 and Supplemental Table 1). There were no subcortical structures that presented significant volumetric reduction in ALS patients. Only the left hippocampus showed a trend towards volumetric reduction ($p = 0.004$, uncorrected) in those patients. VBM analysis found volumetric GM reduction in patients with ALS at the Right Middle Frontal Gyrus, Left Inferior Frontal Gyrus, Left Medial Frontal Gyrus, and both Precentral Gyri.

3.2.2. Longitudinal

FreeSurfer longitudinal analyses only showed progressive reduction of brainstem volumes ($p = 0.00136$, FDR corrected). Such reduction, however, did not correlate with change in clinical scores (including ALSFRSr bulbar subscore). Longitudinal VBM analyses failed to identify regions with progressive volumetric reduction among patients.

3.3. Cerebral WM

3.3.1. Cross sectional

Cross sectional results showed diffuse FA reduction and RD and MD elevation (Fig. 4a, b and c) in patients with ALS compared to healthy controls, especially at the CST and corpus callosum (CC). FA, MD and RD values correlated significantly with ALSFRS-R scores, considering age and gender as covariates (Fig. 4). FA was positively correlated with clinical scores, whereas MD and RD had a negative correlation.

3.3.2. Longitudinal

Longitudinal analyses have shown progressive AD and MD increase (Fig. 4g and h) mostly at the CC in the ALS group. There was no significant change in the control group over time. The change in diffusivity parameters did not correlate with change in ALSFRS-R score or disease duration.

3.4. SC morphometry

We found significant SC atrophy in the ALS group compared to healthy controls (62.0 ± 7.7 mm^2 vs 67.9 ± 6.6 mm^2, $p < 0.001$), but no flattening. There was also a significant but weak correlation between CA and ALSFRS-R score ($r = 0.280$, $p = 0.026$) at baseline in the ALS group.

On longitudinal analyses, we had to exclude one patient due to severe motion artifacts. There was progressive CA reduction in the ALS group ($p = 0.002$) (Fig. 5A). There was also a significant correlation of CA change and ALSFRS-R change in the ALS group ($r = 0.309$, $p = 0.038$ – Fig. 5B). During follow-up, patients had a mean 4.7 point decline in the ALSFRS-R score (reduction of 14.8% compared to baseline score),

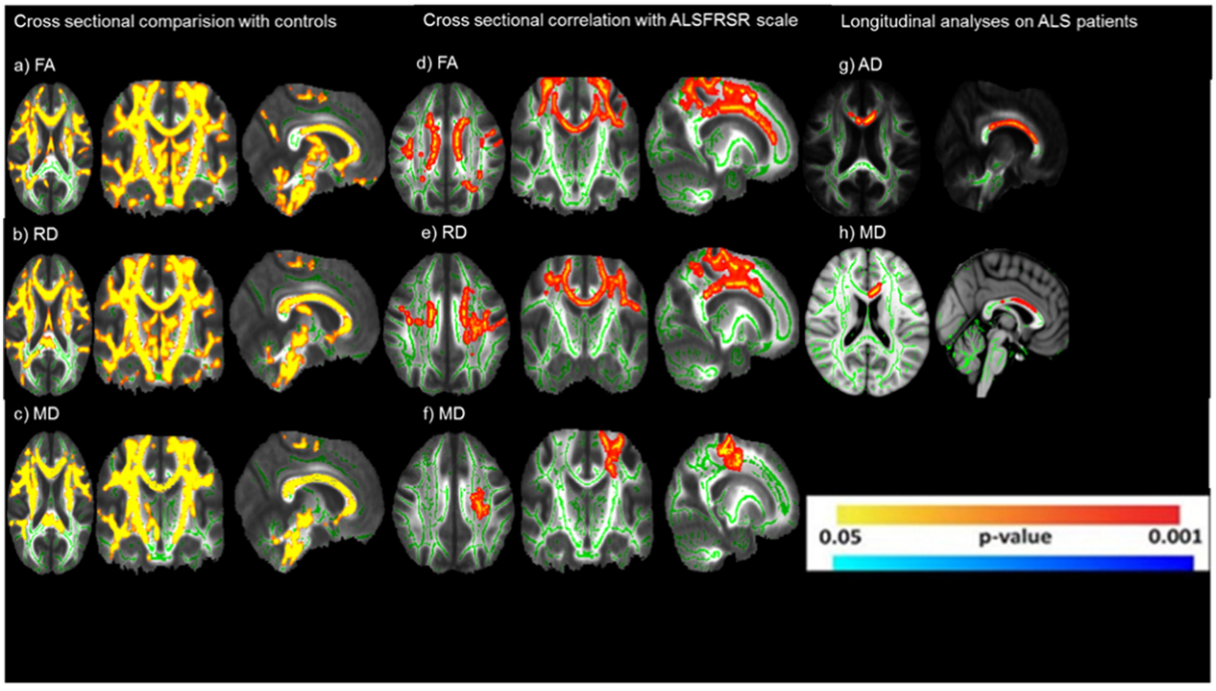

Fig. 4. Results of tract-based spatial statistics showing regions with significant diffusivity abnormalities in patients with ALS when compared to healthy controls. (a, b, c) in cross sectional analyses. Correlation with ALSFRSR in cross sectional analyses (d, e, f) Longitudinal analyses in ALS group (g, h).

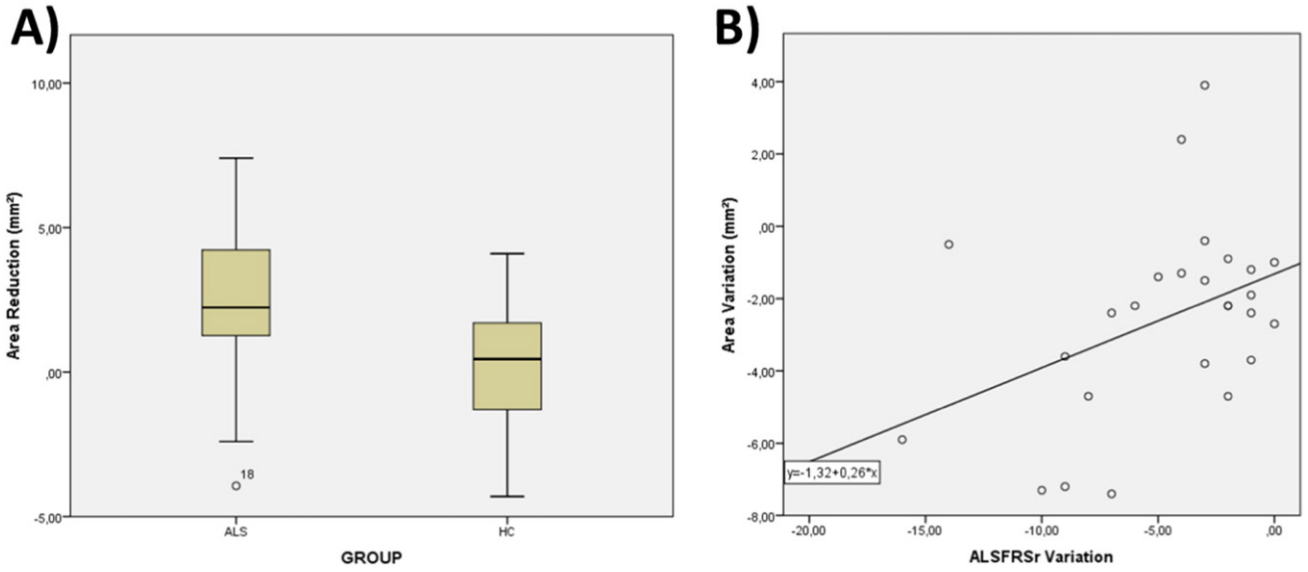

Fig. 5. Spinal cord area longitudinal results: (A) Box and whiskers plot showing area variation after 8 months in the ALS and healthy control groups. (B) Scatter plot showing the correlation between area variation (y-axis) and clinical decline (x-axis).

and a mean reduction of 2.6 mm^2 in CA (reduction of 4.0% compared to baseline CA).

3.5. Change rate of different parameters

SRM of all MRI parameters that presented significant longitudinal change are depicted in Fig. 6.

4. Discussion

Pathological studies in ALS identified a pattern of diffuse cerebral GM degeneration, especially at primary motor areas (Meadowcroft et al., 2015; Smith, 1960) and frontotemporal regions (Smith, 1960). Our cross-sectional findings are in agreement with those reports, and also with previous MRI-based studies (Verstraete et al., 2012; Walhout et al., 2014). We indeed found extensive GM loss at precentral, paracentral as well the temporal regions. Similar to previous studies, we identified slightly asymmetric abnormalities; CT reduction was most prominent at the right cerebral hemisphere, mostly at the precentral gyrus. We did not find subcortical atrophy in ALS patients, which is in line with most other studies that employed the FreeSurfer segmentation protocol (Agosta et al., 2012; Verstraete et al., 2012). Furthermore, we have failed to show a significant correlation between GM damage and clinical parameters, represented here by ALSFRS-R global scores. Verstraete et al. (2015) already discussed this lack of correlation between imaging parameters and clinical metrics, reported across ALS imaging studies. In contrast, we found progressive brainstem atrophy in the follow-up, which has not been previously reported, but this is consistent with the disease pathophysiology. Despite the worsening of the clinical scale and the obvious progression of the disease, this technique found very subtle progression and only in the brainstem. This may be related to a floor effect since our patients already had 30 months of disease duration when first assessed. At this disease stage, it is probable that severe cortical damage already took place and this would make it hard to identify further progression.

Extensive cerebral WM degeneration is a hallmark of ALS, specially at the CST, CC and frontotemporal regions according to autopsy (Smith, 1960) and neuroimaging studies (Roccatagliata et al., 2009; Zhang et al., 2011). We have indeed confirmed an extensive pattern of diffusivity abnormalities, which is probably linked to the loss of WM

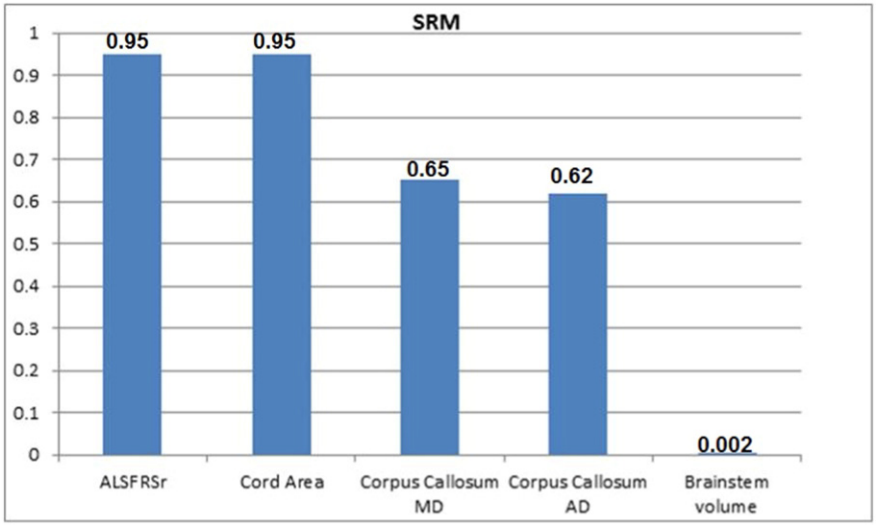

Fig. 6. Standardized response mean (SRM) of different clinical and MRI parameters in patients with ALS.

fibre integrity. Such WM damage correlated with clinical scores. We have chosen the TBSS method instead of targeted tractography (employed in most previous studies (Roccatagliata et al., 2009; Zhang et al., 2011)) because it is an automated method, with higher reproducibility and properly designed for exploratory whole-brain analyses. Follow-up data showed progressive diffusivity abnormalities mostly at the CC. Previous longitudinal MRI-based studies in ALS have controversial findings regarding progression of WM damage, especially at the CST. In one study with 17 patients, FA of the right superior CST was reduced at baseline and such FA change declined significantly over time (Zhang et al., 2011). Another study also with 17 patients found FA reduction of the CST, insula, ventrolateral premotor cortex in cross-sectional analyses, but DTI abnormalities extended mainly into bilateral frontal lobes (Senda et al., 2011). We hypothesize that major caveats in those studies were the reduced number of individuals on follow-up analyses and the approach employed to assess longitudinal changes (Senda et al., 2011; Zhang et al., 2011). Interestingly, a previous study that used the longitudinal TBSS pipeline reported results very similar to our own (Menke et al., 2014).

Neuroimaging methods are potential candidates to identify longitudinal biomarkers in ALS. In this scenario, it is of utmost importance to assess which MRI parameters are more sensitive to detect longitudinal changes in ALS. In the same cohort of patients, we were able to show that spinal cord morphometry and DTI-based metrics were more sensitive than cortical thickness measurements. Overall, these findings suggest that the quantification of damage at the distal portions of the motor system might be more interesting in the long term.

SC segmentation and measurements were performed semi-automatically using the SpineSeg software tool, developed at UNICAMP and previously validated (Bergo et al., 2012; Chevis et al., 2013). This software performs SC morphometric analyses using slightly modified brain MRI acquisitions; it does not require a specific SC MRI protocol, which makes it suitable for routine clinical application. Considering all methods, the functional clinical score is still the most sensitive to show longitudinal changes. However, taking only MRI-based data into account, SC morphometry appears to be the most sensitive parameter. Moreover, the only MRI parameter that correlated with clinical deterioration was precisely CA decline. A previous MRI-based study that evaluated MRI in ALS found significant decrease in cord area in cross-sectional evaluation and in follow-up analysis (Agosta et al., 2009). These results reinforce the potential usefulness of SC morphometry for longitudinal studies and clinical trials. The association of novel techniques such as DTI and ^{1}H-MRS might increase the value of SC MRI in ALS and should be investigated in future studies.

We must acknowledge that this study has some important limitations. One of these is the high rate of drop out for longitudinal studies. Although this is a common finding in prospective studies with ALS (due to the ominous disease course), it reduces the power of our sample to detect longitudinal changes. We believe that the TBSS pipeline for longitudinal assessment of WM is valuable and has been employed in other studies (Menke et al., 2014; Rezende et al., 2016). Nevertheless, it does not account for group vs time interactions because comparisons rely upon paired *t*-tests. Despite that, we believe that our results provide valid insights into disease course, and especially enable the proper comparison of different neuroimaging methods in the context of ALS.

5. Conclusions

Structural MRI is able to detect prospective changes in ALS after 8 months of follow-up, mainly at the corpus callosum and cervical cord. In addition, spinal cord area was the most sensitive MRI parameter to detect longitudinal change and the single one that correlated with clinical deterioration. Overall, these results point to the potential usefulness of spinal cord morphometry as a clinical marker in ALS. Further larger prospective studies should be done to assess the functional correlates of such cord damage.

Supplementary data to this article can be found online at http://dx.doi.org/10.1016/j.nicl.2017.01.024.

Study funding

Supported by FAPESP (grant 2011/21521-3).

Disclosures

Dr. Albuquerque received a PhD scholarship from FAPESP.
Dr. Branco received a PhD scholarship from CAPES.
Dr. Rezende received a PhD scholarship from FAPESP.
Dr. Andrade reports no disclosures.
Dr. Nucci reports no disclosures.
Dr. França Jr. received research support from CNPq and FAPESP.

Acknowledgements

Study funding by Sao Paulo Research State Foundation FAPESP (Grant 2011/21521-3 and 2013/07559-3).

References

Agosta, F., Rocca, M.A., Valsasina, P., et al., 2009. A longitudinal diffusion tensor MRI study of the cervical cord and brain in amyotrophic lateral sclerosis patients. J. Neurol. Neurosurg. Psychiatry 80, 53–55.
Agosta, F., Valsasina, P., Riva, N., et al., 2012. The cortical signature of amyotrophic lateral sclerosis. PLoS One 7 (e42816), 1–8.
Ashburner, J.A., 2007. A fast diffeomorphic image registration algorithm. NeuroImage 38, 95–113.
Ashburner, J., Friston, K.J., 2000. Voxel-based morphometry – the methods. NeuroImage 11, 805–821.
Bede, P., Byrne, S., Mclaughlin, R.L., et al., 2013. Basal ganglia involvement in amyotrophic lateral sclerosis. Neurology 2107–2115.
Bergo, F.P.G., França Jr., M.C., Chevis, C.F., Cendes, F., 2012. SpineSeg: a segmentation and measurement tool for evaluation of spinal cord atrophy. CISTI'2012 (7 ª Conferencia Ibérica de Sistemas y Tecnologia de Información). IEEE, Madrid, Spain, pp. 400–403.
Bernal-Rusiel, J.L., Greve, D.N., Reuter, M., Fischl, B., Sabuncu, M.R., 2013. Statistical analysis of longitudinal neuroimage data with Linear Mixed Effects models. NeuroImage 66, 249–260.
Branco, L.M.T., De Albuquerque, M., De Andrade, H.M.T., Bergo, F.P.G., Nucci, A., França, M.C., 2014. Spinal cord atrophy correlates with disease duration and severity in amyotrophic lateral sclerosis. Amyotroph. Lateral Scler. Frontotemporal Degener. 15, 93–97.
Brooks, B.R., Miller, R.G., Swash, M., Munsat, T.L., 2000. El Escorial revisited: revised criteria for the diagnosis of amyotrophic lateral sclerosis. Amyotroph. Lateral Scler. Other Motor Neuron Disord. 1, 293–299.
Buckner, R.L., Head, D., Parker, J., et al., 2004. A unified approach for morphometric and functional data analysis in young, old, and demented adults using automated atlas-based head size normalization: reliability and validation against manual measurement of total intracranial volume. NeuroImage 23, 724–738.
Cardenas-Blanco, A., Machts, J., Acosta-Cabronero, J., Kaufmann, J., Abdulla, S., Kollewe, K., Petri, S., Schreiber, S., Heinze, H.J., Dengler, R., Vielhaber, S., Nestor, P.J., 2016. Structural and diffusion imaging versus clinical assessment to monitor amyotrophic lateral sclerosis. Neuroimage Clin. 11, 408–414.
Cedarbaum, J.M., Stambler, N., Malta, E., et al., 1999. The ALSFRS-R: a revised ALS functional rating scale that incorporates assessments of respiratory function. J. Neurol. Sci. 169, 13–21.
Chevis, C.F., da Silva, C.B., D'Abreu, A., et al., 2013. Spinal cord atrophy correlates with disability in Friedreich's ataxia. Cerebellum 12, 43–47.
De Albuquerque, M., Anjos, L.G.V., Maia Tavares de Andrade, H., et al., 2016. MRI texture analysis reveals deep gray nuclei damage in amyotrophic lateral sclerosis. J. Neuroimaging 26, 201–206.
Desikan, R.S., Ségonne, F., Fischl, B., et al., 2006. An automated labeling system for subdividing the human cerebral cortex on MRI scans into gyral based regions of interest. NeuroImage 31, 968–980.
Fischl, B., Dale, A.M., 2000. Measuring the thickness of the human cerebral cortex from magnetic resonance images. Proc. Natl. Acad. Sci. U. S. A. 97, 11050–11055.
Fischl, B., Salat, D.H., Busa, E., et al., 2002. Whole brain segmentation: automated labeling of neuroanatomical structures in the human brain. Neuron 33, 341–355.
Foerster, B.R., Welsh, R.C., Feldman, E.L., 2013. 25 Years of neuroimaging in amyotrophic lateral sclerosis. Nat. Rev. Neurol. 9, 513–524 Nature Publishing Group.
Gläscher, J., Gitelman, D., 2008. Contrast weights in flexible factorial design with multiple groups of subjects. https://www.jiscmail.ac.uk/cgibin/webadmin?A2=ind0803&L=SPM&P=R1 6629.
Holtbernd, F., Eidelberg, D., 2014. The utility of neuroimaging in the differential diagnosis of parkinsonian syndromes. Semin. Neurol. 34, 202–209.
Kazis, L.E., Anderson, J.J., Meenan, R.F., 1989. Effect sizes for interpreting changes in health status. Med. Care 27, S178–S189.

Kiernan, M.C., Vucic, S., Cheah, B.C., et al., 2011. Amyotrophic lateral sclerosis. Lancet 377, 942–955.
Meadowcroft, M.D., Mutic, N.J., Bigler, D.C., et al., 2015. Histological-MRI correlation in the primary motor cortex of patients with amyotrophic lateral sclerosis. J. Magn. Reson. Imaging 41, 665–675.
Menke, R.A.L., Körner, S., Filippini, N., et al., 2014. Widespread grey matter pathology dominates the longitudinal cerebral MRI and clinical landscape of amyotrophic lateral sclerosis. Brain 137, 2546–2555.
Reuter, M., Rosas, H.D., Fischl, B., 2010. Highly accurate inverse consistent registration: a robust approach. NeuroImage 53, 1181–1196.
Reuter, M., Fischl, B., 2011. Avoiding asymmetry-induced bias in longitudinal image processing. NeuroImage 57, 19–21.
Reuter, M., Schmansky, N.J., Rosas, H.D., Fischl, B., 2012. Within-subject template estimation for unbiased longitudinal image analysis. NeuroImage 61, 1402–1418.
Rezende, T.J., Silva, C.B., Yassuda, C.L., Campos, B.M., D'Abreu, A., Cendes, F., Lopes-Cendes, I., França Jr., M.C., 2016. Longitudinal magnetic resonance imaging study shows progressive pyramidal and callosal damage in Friedreich's ataxia. Mov. Disord. 31, 70–78.
Roccatagliata, L., Bonzano, L., Mancardi, G., Canepa, C., Caponnetto, C., 2009. Detection of motor cortex thinning and corticospinal tract involvement by quantitative MRI in amyotrophic lateral sclerosis. Amyotroph. Lateral Scler. 10, 47–52.
da Rocha, A.J., Maia Júnior, A.C.M., 2012. Is magnetic resonance imaging a plausible biomarker for upper motor neuron degeneration in amyotrophic lateral sclerosis/primary lateral sclerosis or merely a useful paraclinical tool to exclude mimic syndromes? A critical review of imaging applicability. Arq. Neuropsiquiatr. 70, 532–539.
Salvatore, C., Cerasa, A., Battista, P., Gilardi, M.C., 2015. Magnetic resonance imaging biomarkers for the early diagnosis of Alzheimer's disease: a machine learning approach. Front. Neurosci. 9, 1–13.
Schuster, C., Elamin, M., Hardiman, O., et al., 2015. Presymptomatic and longitudinal neuroimaging in neurodegeneration—from snapshots to motion picture: a systematic review. J. Neurol. Neurosurg. Psychiatry 86, 1089–1096.
Senda, J., Kato, S., Kaga, T., et al., 2011. Progressive and widespread brain damage in ALS: MRI voxel-based morphometry and diffusion tensor imaging study. Amyotroph. Lateral Scler. 12, 59–69.
Smith, M.C., 1960. Nerve fibre degeneration in the brain in amyotrophic lateral sclerosis. J. Neurol. Neurosurg. Psychiatry 23, 269–282.
Smith, S.M., Jenkinson, M., Johansen-Berg, H., et al., 2006. Tract-based spatial statistics: Voxelwise analysis of multi-subject diffusion data. NeuroImage 31, 1487–1505.
Smith, S.M., Nichols, T.E., 2009. Threshold-free cluster enhancement: addressing problems of smoothing, threshold dependence and localisation in cluster inference. NeuroImage 44, 83–98.
Talairach, J., Tournoux, P., 1988. Co-planar Stereotaxic Atlas of the Human Brain. Thieme, NY.
Turner, M.R., Agosta, F., Bede, P., Govind, V., Lulé, D., Verstraete, E., 2012. Biomark. Med. Jun 6 (3), 319–337.
Turner, M.R., Kiernan, M.C., Leigh, P.N., Talbot, K., 2009. Biomarkers in amyotrophic lateral sclerosis. Lancet Neurol. 8, 94–109.
Turner, M.R., Bowser, R., Bruijn, L., et al., 2013. Mechanisms, models and biomarkers in amyotrophic lateral sclerosis. Amyotroph. Lateral Scler. Frontotemporal Degener. 14, 19–32.
Verstraete, E., Veldink, J.H., Hendrikse, J., Schelhaas, H.J., van den Heuvel, M.P., van den Berg, L.H., 2012. Structural MRI reveals cortical thinning in amyotrophic lateral sclerosis. J. Neurol. Neurosurg. Psychiatry 83, 383–388.
Verstraete, E., Turner, M.R., Grosskreutz, J., Filippi, M., Benatar, M., 2015. attendees of the 4th NiSALS meeting. Mind the gap: the mismatch between clinical and imaging metrics in ALS Amyotroph Lateral Scler Frontotemporal Degener. 6 (7-8), 524–529.
Walhout, R., Westeneng, H.-J., Verstraete, E., et al., 2014. Cortical thickness in ALS: towards a marker for upper motor neuron involvement. J. Neurol. Neurosurg. Psychiatry 86, 1–7.
Westeneng, H.-J., Verstraete, E., Walhout, R., et al., 2015. Subcortical structures in amyotrophic lateral sclerosis. Neurobiol. Aging 36, 1075–1082.
Zhang, Y., Schuff, N., Woolley, S.C., et al., 2011. Progression of white matter degeneration in amyotrophic lateral sclerosis: a diffusion tensor imaging study. Amyotroph. Lateral Scler. 12, 421–429.